Indian Journal of Pure & Applied Physics
Vol. 59, May 2021, pp. 379-385

Experimental Investigation of Mechanical and Thermal Study of Mg/B_4C/Cr Hybrid Composites

Sakshi Singh* & Nathi Ram Chauhan

Mechanical and Automation Engineering Department

Indira Gandhi Delhi Technical University for Women, New Church Rd, Opp. St, Kashmere Gate, New Delhi, Delhi 110 006 India

Received 2 July 2020; accepted 25 March 2021

This study explores the investigation of enhanced mechanical and thermal properties of Mg/B4C/Cr hybrid composites having varying 3, 5, 7 wt. % of B_4C and Cr reinforcements in Mg-matrix. The bottom pouring vacuum-based squeezed stir casting process is used to fabricate these composites. The Mg/B_4C/Cr hybrid composites evaluate ultimate strength, elongation percentage, expansion coefficient, heat conductivity, hardness, and then compared with Mg/5B_4C and Mg/5Cr composites. Each of Mg-based hybrid composites results indicates higher thermal conductivity and expansion coefficient than Mg/5B_4C and Mg/5Cr composites. The tensile results reveal that the Mg/B_4C/Cr hybrid composites show mixed morphologic behaviour of brittle-ductile while Mg/5B_4C and Mg/5Cr composites are individually evident with brittle behaviour. The proper interfaces between Cr particles and Mg matrix illustrate reduced dislocations with efficient strength and thermal results. However, B_4C particles present in the base matrix is liable for the effective hardness and ultimate strength in the Mg/B_4C/Cr hybrid composites. In comparison with other composites (Mg/B_4C and Mg/Cr), Mg/B_4C/Cr hybrid composite shows efficient thermal conductivity with high thermal conductance which diverges towards the application of gas cylindrical liners.

Keywords: Hybrid Composites, Mechanical Properties, Thermal Properties, B_4C Particles, Chromium, Stir Casting

1 Introduction

For two decades, Mg-based composites by ceramics/carbide particles have been evolved as leading competitor materials in various applications because of its low density (1.732g/cm^3), and good specific strength[1]. Most of its application required good mechanical, thermo-physical and corrosion-resistant properties simultaneously[2]. Mostly, carbide and ceramics reinforcements are used in Mg matrix composites and its alloys because of its excellent thermo-physical properties and specific strength. However, sometimes carbide particles show weak interfacial bonding due to its chemical reactivity (low corrosion resistance) which causes dislocations in the interfaces of composite matrix. These dislocations create plasticity and interfacial degradation. As a result, it is hard to accomplish excellent thermal and mechanical properties of carbides based Mg composites. Moreover, few methods could improve the thermo-physical properties of Mg-based composites such as metallization of the surface by adding reinforcements (such as Cr, SiC, Ti)[3-5] and addition of alloy as a base matrix with metal materials (such as TiC, Si, B_4C)[6-8]. But previous studies are only focussing on the improvement of strengthening properties of Mg-based composites and not on thermo-physical properties which have been remarked rarely[9-11]. The up-gradation of amorphous and metallic particles such as TiC, graphite, alumina has been investigated based on the requirements in the applications involving strengthening properties of Mg and its alloys [12-16]. The study of such reinforcements could exhibit the favourable interfacial properties but the absence of thermo-physical properties as compared to carbide with Mg-based matrices.

Kumar *et al.* [17] investigates the review study on light-weight cylindrical liners. Their study represents the development of cylindrical liners would be possible by Mg-matrix with graphite and Mg alloy with SiC composites by stir casting route. Furthermore, Olufemi *et al.*[18] indicate the Al-Mg based alloys are also applicable for cylindrical liners and frames. Although in the literature review, the cylindrical liners are generally reviewed on Al and its alloys due to its remarkable properties when fabricated with reinforcement. But very rare studies have been observed with Mg and its alloys.

*Corresponding author : (E-mail : singh.sakshi0408@gmail.com)

Processing methods would surely upgrade the mechanical and thermal properties of Mg-based matrix composites due to its adequate stability between mechanical and thermal bonding under different conditions[19]. Favourably, Shamshekh *et al.*[20] also describe the inclusion of nano-Ti particulates in Mg-based composites which enhanced the strengthening properties and heat conductivity of Mg-based composites using the powder metallurgy method. Although, when the same composite amalgamates by stir casting method, both carbide and metallic reinforced particles show effective mechanical and corrosion-resistant properties.

Compared to carbide particles, B_4C (density: 2.52 g/cm^3) is having high hardness and modulus as well as good thermal conductivity value[21]. Thus mostly, B_4C is preferred as reinforcement material. However, chromium is usually preferred for coating the materials to improve the service life and corrosion-resistant properties of composites[22]. The anticipation of a small fraction of chromium particulates in the metal matrix also results in improved microstructural interfacial bonding[23]. Nevertheless, Mg ingots have been selected as a matrix material for fabrication of composites, because of its low cost and availability in the majority of industrial areas as a raw material in comparison to other Mg-alloys.

Consequently, from the above literature review, confined results have been recorded on the thermal properties of Mg-based composites. Thus this paper focuses on two objectives. Firstly, enhanced the thermal properties of each hybrid composites having Mg as a base matrix and compared with each other. Secondly, a thorough investigation of the effect of reinforced Cr particles on metallographic and strengthening properties using weight fraction of B_4C reinforced Mg-based composites.

2 Experimental

The Mg hybrid composites (B_4C + Cr) have been fabricated by blending of boron carbide (250 μm) and chromium (60 μm) particles using vacuum-based (bottom pouring) squeezed stir casting process having varying weight fraction percentage of 3, 5, and 7.

Initially, to remove the moisture contents from reinforced particles, B_4C and Cr powders have been placed in an electric oven at 250 ^oC separately. Then under continuous stirring, the matrix metal (Mg ingots) is placed in a vacuum-based preheated muffle furnace with a supply of argon with SF_6 cover gas to extinguish from fire. Then reinforcements (B_4C+Cr) have been dropped into the molten melt of Mg with continuous stirring. About 750-850 ^oC of stirring temperature and constant 450 rpm of stirring speed has been applied to the setup to attain homogeneous arrangement. After 10-15 minutes of stirring, the composite melt has been dropped into the mould by the bottom pouring approach. In the bottom pouring approach, a preheated small inclined runway (300 ^oC) is attached at the bottom of the muffle furnace to maintain the temperature of the composite melt. Then the composite melt is poured into the mould and instantaneously squeeze pressure (250 MPa) is applied by the hydraulic press for a few minutes to remove the residual defects. After solidifying at room temperature, fabricated specimens have been taken out from the mould and slice out as per testing dimensions.

By the multiplication of thermal data values (such as density, specific heat capacity, thermal diffusivity), the heat conductivity of Mg-based composites has been calculated. A thermo-mechanical analyser integrated with laser flash (NPL, Delhi) is preferred for evaluation of heat capacity, density (by Archimedes' principle), and thermal expansion coefficient values. The intermediate dimensions of the specimen are in disc form having 5-12 mm of diameter with 1-3 mm of thickness with the temperature range varied from RT to 1000 ^oC at a rate of 5 $^oC/min^{-1}$. A diffraction meter (JMI, Center of Nanoscience and Nanotechnology, Delhi) is tested for phase study of Mg-based composites upto 80 degrees at a speed of 2deg/min. The metallographic studies of composites have been analyzed in a metallurgical electron microscope (JMI, Central Instrumentation Facility, Delhi). The Rockwell hardness tests (JMI, ME Department, Delhi) have been performed on Rockwell hardness tester applying a load of 100 kgf for 15 seconds and the average value of hardness is used for analysis purpose. The dimensions of these test specimens are 10×10×10 mm in solid cubical form. The tensile test has been performed on tensometer (JMI, ME Department, Delhi) at normal temperature with the transverse speed of 1m/sec. The tensile specimens have been prepared as per ASTM B557M–15 standards in dog-bone type shape[24].

Thus, these Mg-based B_4C-reinforced composites are machined to investigate the significance of Cr reinforcement on mechanical and thermal results.

3 Results

3.1 Microstructure

The microstructural images of Mg/B_4C/Cr hybrid composites as represent in Figs. 1(a-c). The images show B_4C and Cr reinforcements are homogeneously dispersed in the Mg-based where bright colour represents Cr along with dark patches gives the evident of boron carbide particles. Besides, the grey phase depicts Mg-base matrix having no distinct interfaces. However, the microstructural images of Mg/5B_4C and Mg/5Cr composites also show the homogeneous dispersion of B_4C and Cr reinforcements in the Mg-based matrix.

Each of the microstructural images reveals the presence of few microstructural defects such as porosity and white inclusion. As shown in Table 1, the formation of microstructural defects is due to the considerable variations in each of the thermal coefficient values of the Mg, B_4C and Cr materials in Mg-based composites.

Another reason is the occurrence of porosity due to entrapment of gases during liquefaction of composite into the melt whereas white inclusion occurs due to the oxidation reaction of Mg-matrix during the fabrication process. These defects are confirmed by the variation in the porosity values as shown in Table 2. The variation in the porosity values affects the microstructural characteristics considerably[25].

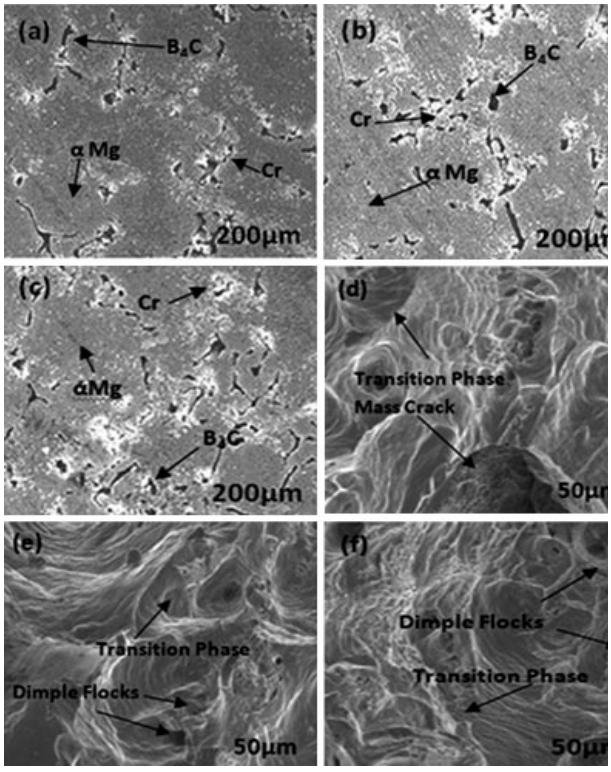

Fig. 1 — Microscopic Results (a-c) and Fractographic Results (d-f) of Mg/B_4C/Cr based Hybrid Composites: (a) & (d) Mg/7B_4C/3Cr, (b) & (e) Mg/5B_4C/5Cr and (c) & (f) Mg/3B_4C/7Cr

3.2 Diffraction Patterns

The diffraction patterns of Mg/B_4C/Cr hybrid composites indicate well retention of Cr particles with the proper amalgamation of B_4C particles in the Mg-matrix. While Fig. 2 represents the formation of small peaks of B_4C and Cr in the Mg/5B_4C/5Cr composite in different forms of phases. However, diffraction patterns of other Mg/B_4C/Cr composites represent quite similar patterns but peaks may vary according to the inclusion of B_4C and Cr weight fraction percentage.

3.3 Hardness

Table 2 and Fig. 3 represents the Rockwell hardness (average) data values of Mg/5B_4C, Mg/5Cr and Mg/B_4C/Cr composites. The nano-indentations are usually measured the geometrical dislocations of the composite interfaces[26]. The Mg/5B_4C composite shows the hardness value of 55HRE while Mg/5Cr composite indicates 44HRE hardness value. However, the Mg/B_4C/Cr hybrid composites evaluate the higher hardness values in comparison to Mg/5B_4C and Mg/5Cr based composites. These results show increment due to the presence of Cr particles along with B_4C contents. This is due to an increase in the formation of the hardening zones around the Mg/B_4C and Mg/Cr interfaces between the particles and the Mg-matrix. Mg/7B_4C/3Cr composite shows the highest hardness value in comparison to other composites. 33% and 46% of hardness are increased in Mg/7B_4C/3Cr hybrid composite compared with B_4C and Cr- based composites respectively due to the inclusion of B_4C and Cr reinforced particles.

Table 1 — Fabricated Composites Compositions and Physical Properties of the Materials Involved

S. No.	Sample No.	Sample Name	B_4C wt.%	Cr wt.%
1.	Sample 1	Mg/5B_4C	5	0
2.	Sample 2	Mg/5Cr	0	5
3.	Sample 3	Mg/7B_4C/3Cr	7	3
4.	Sample 4	Mg/5B_4C/5Cr	5	5
5.	Sample 5	Mg/3B_4C/7Cr	3	7

Materials	Density (g/cm^3)	TC (W/m K)	α (µm/m °C)
Mg	1.73	156	27
B_4C	2.52	72.7	26
Cr	7.15	93.7	6.2

Table 2 — Mechanical and Thermal Properties of Mg Composite Materials

Properties → ↓ Composites	Mg/5B_4C	Mg/5Cr	Mg/7B_4C/3Cr	Mg/5B_4C/ 5Cr	Mg/3B_4C/7Cr
Hardness (HRE)	55	44	83	76	70
Density, ρ (g/cm^3)	1.77	2.00	1.94	2.04	2.13
Porosity	0.58	1.97	2.76	2.55	1.07
UTS (MPa)	199.3	170.63	224	242	246
YS (MPa)	96	86.4	142	159.62	164
Elongation %	1.93	1.86	2.46	2.62	2.61
Elastic Modulus, E	49.06	45.55	57.78	60.94	62.83
TC(W/mK)	146.7	143.4	150.9	148.5	150
α (μm/m ^{o}C)	24.8	24.5	26.9	25.7	26.6
h_c (x10^7 W/m^{2}K)	3.5	3.1	4.7	4.2	4.6

Note: Porosity (%) = (1- Actual Density/Exp. Density) ×100
Elongation % = (Increased Gauge Length- Original Gauge Length/ Original Gauge Length) × 100
UTS- Ultimate Tensile Strength, YS- Yield Strength, TC- Thermal Conductivity
α- Thermal Expansion Coefficient, h_c – Thermal Transmittance

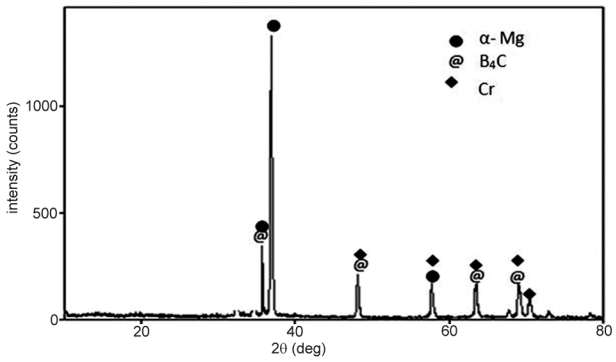

Fig. 2 — Diffraction Results of Mg/5B_4C/5Cr Hybrid Composite

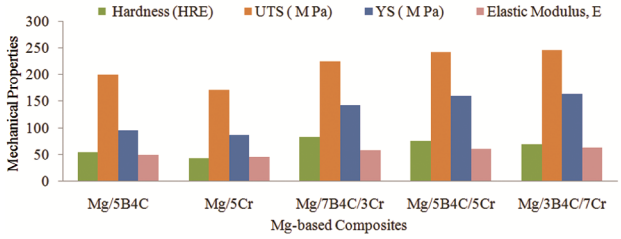

Fig. 3 — Analysis of Mechanical Properties of Mg-based Composites

3.4 Tensile

Figure 3 evaluates the average values of the tensile test results of the Mg matrix composites. The Mg/B_4C/Cr hybrid composites exhibit higher yield strength and elasticity modulus in comparison to Mg/5B_4C and Mg/5Cr composites. The highest ultimate strength of Mg/3B_4C/7Cr composite is 246 MPa which is 18.9% higher than Mg/5B_4C and 30.6% higher than Mg/5Cr composites. However, the value elongation and elastic modulus of Mg/3B_4C/7Cr hybrid composite are 2.61 and 62.83 respectively.

The fractographic images of Mg/B_4C/Cr hybrid composites have been shown in Figs. 1 (d-f). Mg/7B_4C/3Cr composite is having a mass of cracks enclosing between the B_4C and Mg-matrix interfaces which represent brittle transition. This occurs due to the formation of a strong hardening zone and causes delamination of the interfaces due to its addition of high weight percentage of B_4C. However fractographic images of Mg/3B_4C/7Cr and Mg/5B_4C/5Cr hybrid composites represent a mixed morphological behaviour having brittle-ductile transition with Cr fragments having the growth of dimples. These flocks of dimples indicate the deterioration of interfacial bonding in-between B_4C and Mg-based matrix in the composites due to its addition of high weight percentage of Cr. This analysis illustrates that the interfaces in-between Mg/Cr having higher binding stability than Mg/B_4C interfaces which develops a better influence on the strengthening properties of Mg hybrid composites as compared to Mg/5B_4C and Mg/5Cr composites. Thus Mg/B_4C/Cr hybrid composites explain the contribution of better toughness and tolerance failure due to Cr reinforcement than B_4C [27].

Nelson *et al.*[28] also reported the similar formation of diffusion interface layer embedded in Ti-based SiC reinforced Mg-composites, which indicates the development of nano-interfaces which eliminates the crack orientation around the interfaces. Thus leads to enhancement of strengthening and ductile features. Analogously, the result shows that elemental MgO is also found along with Mg/Cr interface which indicates the evolution of a MgO layer and produces improved the interfacial strength. This shows that

mechanical properties of Mg/3B_4C/7Cr hybrid composite have been suitable for the designated Mg-based composites.

3.5 Thermal Effect

Figure 4 and Table 2 represent the thermal properties of Mg-based matrix composites. Figure 4 calculates the thermal expansion values of Mg/B_4C/Cr composites by varying the temperature from 50 to 400 °C. Table 2 shows the (average) varied results of measured thermal values of Mg/B_4C/Cr composites. This is because Mg, B_4C and Cr materials have the variation in between the physical values (as shown in Table 1)which lead to the formation of thermal stress during cooling (fabricating temperature to room temperature). The thermal stresses obtain high concentration effect at Mg/Cr and Mg/B_4C interfaces. However, these concentrations generate microstructural defects in the composite matrix[29].

To investigate the influence of different interface arrangement on thermal conductivity, h_c (interfacial thermal conductance) has been evaluated with the relation with Mg matrix, reinforcements and interface arrangement data.

Hassel mane Johnson model helps to calculate interfacial thermal conductance of Mg/B_4C/Cr composites[30]. According to these equations (Eq.1-3), the interfacial thermal conductance values are calculated as shown in Table 2.

$$1-W_{reinforcement}=\frac{\frac{K^{eff}_{reinforcement}}{K^{eff}_{matrix}}-\frac{K_{composite}}{K^{eff}_{matrix}}}{\frac{K^{eff}_{reinforcement}}{K^{eff}_{matrix}}-1\times\left(\frac{K_{composite}}{K^{eff}_{matrix}}\right)^{-\frac{1}{3}}} \quad \ldots (1)$$

$$K^{eff}_{reinforcement}=\frac{K_{reinforcement}}{1+\frac{K_{reinforcement}}{average\ particle\ size\times h_c}} \quad \ldots (2)$$

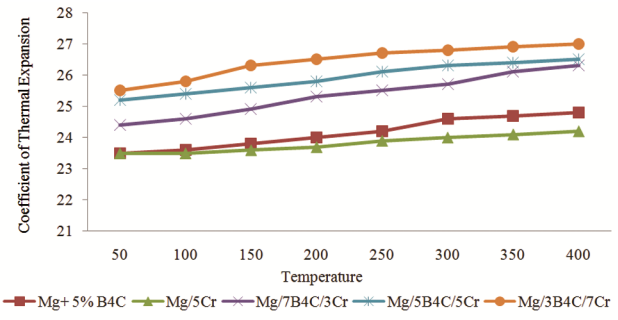

Fig. 4 — Variation of Thermal Expansion values (μm/m° C) with Temperature (° C)

$$K^{eff}_{matrix}=\frac{K_{matrix}\ (2-2V_{pores})}{1+V_{pores}} \quad \ldots (3)$$

Where, K refers to the heat (thermal) conductivity and W refers to the weight fraction. The information about interfacial thermal conductance values is also extracted from the literature studies. Though, interfacial thermal conductance (h_c) indicates the measure of efficient flow of heat from one interface to others. High h_c strikes the effective (eff.) thermal conductivity which results in the reduction in the dislocations with optimum heat dissipation in the composite material[31].

Mg/3B_4C/7Cr evaluates the high thermal conductivity and interfacial thermal conductance values are 150 W/m K, and 4.6X10^7 W/m^2K respectively in comparison to Mg/5B_4C/5Cr hybrid composite. Whereas, $h_c$value of Mg/7B_4C/3Cr hybrid composite is showing the higher value (4.7 × 10^7 W/m^2K) in comparison to other hybrid composites by the increase of B_4C weight fraction.

4 Discussion

To obtain the suitable properties of a composite for the given application, a composite must possess high TC and low thermal expansion value. This means high thermal conductivity contributes to high interfacial thermal conductance (from above equations). However, high thermal conductivity with low expansion value signifies effective thermal effects for Mg-based composite materials. According to the concept of composite material, thermal expansion coefficient (α) and elastic modulus (E) are associated with each other by a mathematical trend of Gruneisen Constant[32]. The Gruneisen Constant formulates as;

$$\alpha=\frac{\gamma_G.\rho.C_v}{3E} \quad \ldots (4)$$

Whereas γ_G is Gruneisen constant which is not a constant but its magnitude is varied from $0.40 < \gamma_G < 4.0$, ρ is the density of the composite material and C_v is the specific heat of the material. This mathematical trend illustrates that if the thermal expansion coefficient value decreases, the elastic modulus increases. However, the modulus of elasticity is strongly influenced by the minimum number of dislocations[33]. Here dislocations imply the microstructural defects (porosity) of the Mg-hybrid composites.

Thus Mg/3B_4C/7Cr composite show high h_c value (4.6×10^7.W/m^2K) which results in high TC (150 W/m K) with low thermal expansion coefficient

(26.6 μm/m^{o}C) as compared to Mg/5B_4C/5Cr hybrid composite. Despite that, under low thermal expansion coefficient, elastic modulus (62.83) is highest for Mg/3B_4C/7Cr composite. This signifies the minimum dislocation *i.e.* porosity (1.07) occurs in Mg/3B_4C/7Cr composite as compared to other Mg/B_4C/Cr hybrid composites. On the other hand, Mg/7B_4C/3Cr composite represents the highest thermal values with reduced elastic modulus having high porosity value. This means a high weight fraction percentage of B_4C affects the thermal properties but decreased the mechanical properties.

Thus, compared with Mg/5B_4C and Mg/5Cr composites, Mg/B_4C/Cr composites possess improved mechanical and thermal properties with the inclusion of Cr and B_4C particles. Meanwhile, in comparison to each of hybrid composites, Mg/3B_4C/7Cr shows an efficient thermal and mechanical property which gives a new diversion toward gas cylindrical liners applications.

5 Conclusions

The Mg/B_4C/Cr composites are strongly developed by Cr and B_4C particles and synthesized by vacuum-based bottom pouring squeeze stir casting. The proper amalgamation (uniform dispersion) of Cr reinforcement exceptionally improved the strengthening and thermal properties of the Mg/B_4C/Cr composites in comparison to Mg/B_4C and Mg/Cr composites. Tensile investigation revealed that the Mg/B_4C/Cr composites having diverse morphologic nature of the ductile-brittle transition. The Mg/7B_4C/3Cr composite attains the highest thermal values and porosity with reduced elastic modulus value. However, an Mg/3B_4C/7Cr composite attains the high thermal conductivity and interfacial thermal conductance with low thermal expansion coefficient which induces high elastic modulus with least porosity value. Thus, comprehensive performances of Mg/3 B_4C/7Cr composite give a source of inclination towards gas cylinder liners applications.

Acknowledgement

Authors acknowledged the University Grant Commission for providing the fellowship amount and (Jamia Millia Islamia and Delhi Technical University) Laboratories for offering the premises for this research work.

References

1 Eacherath S & Murugesan S, *Int J Mater Res*, 109 (2018) 661.

2 Tarafder N & Prasad M L V, *AIP Conf Proc*, 1952 (2018) 020069.

3 Ghasali E, Orooji Y, Alizadeh M & Ebadzadeh T, *Mater Sci Eng A*, 789 (2020), DOI: https://doi.org/10.1016/j.msea.2020.139662.

4 Prakash K S, Balasundar P, Nagaraja S, Gopal P M & Kavimani V, *J Magn Alloys*, 4 (2016) 197.

5 Li Q, Ma Z, Ji S, Song Q, Gong P & Li R, *J Mater Process Technol*, 278 (2020), DOI: https://doi.org/10.1016/j.jmatprotec.2019.116483.

6 Reyes A, Bedolla E, Perez R & Contreras A, *Compos Interf*, 24 (2017) 593.

7 Kaushik N C & Rao R N, *Indus Lubricat Tribol*, 69 (2017) 149.

8 Kumar N, Gautam A, Singh R S & Manoj M K, *Trans Indian Inst Metal*, 72 (2019) 2495.

9 Sardar S, Karmakar S K & Das D, *Mater Today*, 4 (2017) 3280.

10 Kumar A, Kumar S & Mukhopadhyay N K, *J Magn Alloys*, 6 (2018) 245.

11 Meher A, Mahapatra M M, Samal P, Vundavilli P R & Madavan S P, Mater Today, 18 (2019) 4034.

12 Singh S & Chauhan N R, *Int J Microstruct Mater Prop*, 13 (2018) 439.

13 Jiang S, Huang L J, An Q, Geng L, Wang X J & Wang S, J Mech Behav Biomed Mater, 81 (2018) 10.

14 Zhang H, Zhao Y, Yan Y, Fan J, Wang L, Dong H & Xu B, *J Alloys Compd*, 725 (2017) 652.

15 Tian M & Shang C, *Int J Hydrogen Energy*, 44 (2019) 338.

16 Xiao P, Gao Y, Yang X, Xu F, Yang C, Li B & Zheng Q, *J Alloys Compd*, 764 (2018) 96.

17 Kumar P A, Rohatgi P & Weiss D, *Int J Metal Cast*, 14 (2019) 291.

18 Olufemi B P, Oluwaseun K, Christian B, Anthony I, Festus O & Oluropo A, *Manag Sci Eng*, 413 (2018), DOI: https://doi.org/10.1088/1757-899X/413/1/012017.

19 Sakthivelu S, Sethusundaram P P, Meignanamoorthy M & Ravichandran M, *Mech Mech Eng*, 22 (2018) 357.

20 Shamekh M, Pugh M & Medraj M, *Adv Mater Res*, 409 (2012) 215.

21 Du A B, Qu Z X, Su X P & Xiao X, *Key Eng Mater*, 726 (2017) 153.

22 Ju J, Fu H G, Fu D M, Wei S Z, Sang P, Wu Z W & Lei Y P, *Iron-Mak Steelmak*, 45 (2018) 176.

23 Tan Q, Atrens A, Mo N & Zhang M X, *Corrosion Sci*, 112 (2016) 734.

24 Dash D, Singh R, Samanta S & Rai R N, *J Sci Indus Res*, 79 (2020) 164.

25 Ghasali E, Alizadeh M, Shirvanimoghaddam K, Mirzajany R, Niazmand M, Faeghi-Nia A & Ebadzadeh T, *Mater Chem Phys*, 212 (2018) 252.

26 Xu Y, Balint D S & Dini D, Surf Coat Technol, 374 (2019) 763.

27 Oddone V, Boerner B, & Reich S, *Sci Technol Adv Mater*, 18 (2017) 180.

28 Nelson M, Agne M T, Anasori B, Yang J & Barsoum M W, *Mater Sci Eng A*, 705 (2017) 182.

29 Zhu D, Yu W, Du H, Chen L, Li Y & Xie H, *J Nano-Mater*, 2016 (2016), DOI: https://doi.org/10.1155/2016/3089716.

30 Lu T W, Chen W P, Wang P, Mao M D, Liu Y X & Fu Z Q, *J Alloys Compd*, 735 (2018) 1137.

31 Rudajevova A & Lukáč P, *Math Physica*, 41 (2000) 3.

32 Chakraborty S, Islam M R I, Shaw A, Ramachandra L S & Reid S R, *Compos Struct*, 164 (2017) 263.

33 Chand S, Chandrasekhar P, Sarangi R K & Nayak R K, *Materials Today*, 18 (2019) 5356.